Pol. J. Environ. Stud. Vol. XX, No. X (XXXX), 1-13
DOI: *10.15244/pjoes/220561* ONLINE PUBLICATION DATE: 2026-09-23

Original Research

Remediation of Pb-Contaminated Soil with Hydroxyapatite and Potassium Chloride: Performance and Optimization

Xiangyu Bai[1], Xu Xia[2], Xu Han[3], Wenjing Pan[1], Xiaofu Shang[4], Jiachao Jiang[1], Dejun Yang[1], Gongzhen Li[5], Jun Tian[6], Ping Luo[1]*

[1]School of Environment and Spatial Informatics, China University of Mining and Technology, Xuzhou 221116, China
[2]XCMG Xuzhou Truck-mounted Crane Co., Ltd., Xuzhou 221000, China
[3]School of Chinese Language and Literature, Yancheng Teachers University, Yancheng 224002, China
[4]Tianjin Huankelijia Environmental Remediation Technology Co., Ltd., Tianjin 300191, China
[5]State Key Laboratory of Coal Mine Disaster Prevention and Control, China University of Mining and Technology, Xuzhou 221116, China
[6]China Academy of Safety Science and Technology, Beijing 100012, China

Received: 26 December 2025
Accepted: 10 April 2026

Abstract

Hydroxyapatite (HAP) and its modified derivatives represent a feasible approach for remediating lead-contaminated soils, while concerns remain regarding their long-term stability. This study conducted a lab-scale experiment to investigate the synergistic remediation of lead-contaminated soil by HAP and KCl, aiming to efficiently immobilize lead and achieve long-term stabilization. The optimum P:Cl:Pb ratio and the remediation mechanisms were first investigated using the toxicity characteristic leaching procedure, the sequential extraction procedure, and X-ray photoelectron spectroscopy. The 50-year stability was then assessed by conducting simulated exposure to different types of rainfall (SO_4^{2-}:NO_3^- = 1:1, 2:1, and 4:1; pH = 4.5, 5.6, and 6.5). The results showed that after 14 days of treatment, the optimum mixture of HAP and KCl (P:Cl:Pb = 8:2:1, 3.2 wt% HAP) completely immobilized Pb in soil (4985 mg kg^{-1} Pb), generating 49% stable residual Pb. The presence of KCl enhanced the Pb immobilization through the formation of $Pb_5(PO_4)_3Cl$ and $Pb_{10}(PO_4)_6(OH)_2$. Following an additional 50-year simulated rainfall period, the residual Pb fraction further increased to 90%, while the leached Pb concentration remained below the regulatory threshold of 5 mg L^{-1} (GB 5058.3-2007). These findings indicate successful long-term Pb immobilization for at least 50 years, especially under rainfall conditions.

Keywords: Pb immobilization, HAP composite, soil remediation, Pb species distribution, rainfall resistance

*e-mail: ping.luo@live.cn
Tel: +86-15050828650

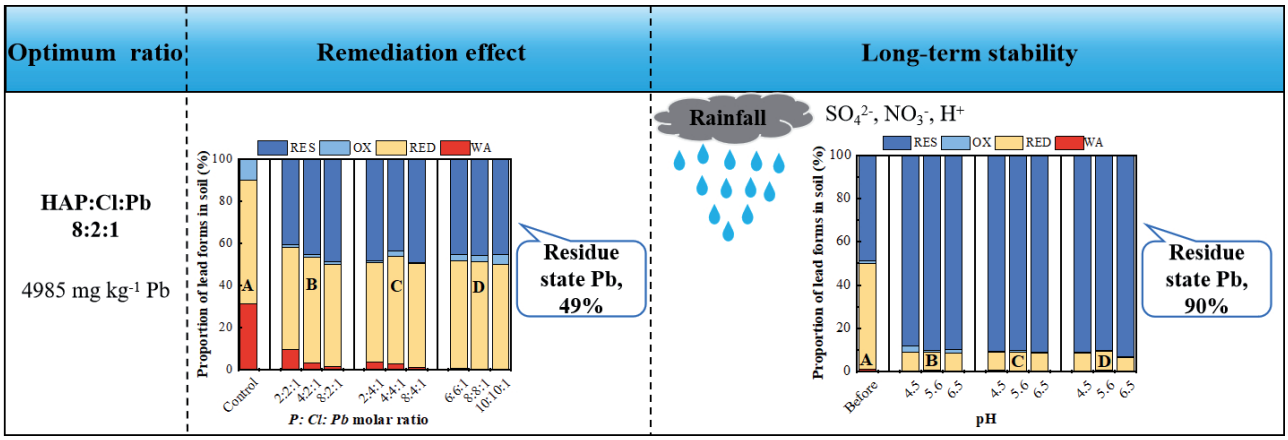

Graphical abstract

Introduction

Due to excessive lead (Pb)-related anthropogenic activities, such as mining, smelting, and agricultural practices, approximately 783,000 metric tonnes of Pb are released into the environment annually [1, 2], leading to the contamination of over 20 million hectares of soil globally [3]. Elevated soil Pb levels severely affect plant metabolism [4, 5] and morphophysiological features, reducing crop growth [6, 7], and ultimately causing neurological and cardiovascular risks to humans via the food chain [8, 9].

Many remediation methods have been developed to mitigate Pb hazards in soil, including physical, biological, and chemical techniques [10-13]. Physical remediation involves soil replacement [14], isolation embedding, and electrokinetic remediation [15], which are simple but costly for large-scale remediation and may disrupt soil structure [16]. The biological techniques, including phytoremediation [17] and bioremediation [18] via fungi and bacteria, immobilize Pb as more stable compounds and reduce its bioavailability [11, 19]. However, phytoremediation is time-consuming and only suits lightly contaminated fields, while fungi and bacteria are vulnerable to soil conditions, and the investigations are still limited to a laboratory scale [20]. Chemical stabilization can convert Pb into insoluble, immobile, and less toxic forms via cation exchange, complexation, precipitation, physisorption, and/or electrostatic interaction [21, 22]. It gained widespread attention in recent decades since it is simple, fast, and cost-effective. Various exogenous materials were explored for Pb remediation [23], such as blast furnace slag, fly ash, sodium sulfide, and natural and biological apatite [22, 24-26].

It is reported that hydroxyapatite (HAP, $Ca_{10}(PO_4)_6(OH)_2$) can immobilize metals via cation exchange, adsorption, surface complexation, precipitation, and co-precipitation [27-30]. Its hexagonal crystal structure provides high ion exchange capacity, allowing Ca^{2+} exchange with metals [31, 32]. The large surface area supplies numerous adsorption points [33, 34]. Moreover, the alkalinity of HAP can promote precipitation, transforming weakly bound, reducible, oxidizable, and water-soluble Pb into pyromorphites, $Pb_{10}(PO_4)_6(OH)_2$, and subsequently reducing the mobility of Pb [35]. However, some of the Pb-HAP-derived products are at risk of being re-released under the influence of environmental factors [36, 37]. This drawback highlights the necessity of finding an additive that can not only reduce costs but also enhance Pb stabilization in the long term.

To find such an additive, the subgroup of pyromorphites, such as $Pb_{10}(PO_4)_6(OH)_2$, $Pb_5(PO_4)_3Br$, and $Pb_5(PO_4)_3F$, was evaluated [38]. It was noted that $Pb_5(PO_4)_3Cl$ has the lowest solubility ($K_{sp} = 10^{-84.4}$) [39], as well as the greatest stability due to its chemical and physical attributes [40, 41]. Therefore, Pb immobilization via the formation of $Pb_5(PO_4)_3Cl$ is plausible and can reduce Pb and phosphorus leaching over time, enhancing long-term stability. However, excessive chloride may erode and deteriorate the hydrated products in the soil, affecting the physical properties of the soil and the effectiveness of remediation [42]. Screening the optimum P:Cl:Pb molar ratio is the key to successful Pb-contaminated soil remediation, which involves testing different ratios to find the best one for Pb immobilization. To the best of our knowledge, this has not been explored so far. Furthermore, after reviewing the bibliography on Pb-contaminated soil remediation using HAP-related materials, no research data on its long-term stability have been published so far [32, 35, 43-46].

This study aims to evaluate the optimum ratio, mechanisms, long-term stability, and cost-effectiveness of synergistic remediation of Pb-contaminated soils using hydroxyapatite combined with chloride. Potassium chloride (KCl) was selected as the chloride source since it is cheap and widely available on the market [40, 43]. The risk assessment code (RAC) was calculated to assess the environmental risks of Pb exposure at different remediation stages. It is worth mentioning that this paper focuses on the evaluation of the combined effect of HAP and KCl. The single effect of HAP was ignored

Table 1. The physical and chemical properties of natural and Pb-contaminated soil. All tests were conducted in triplicate.

Properties	Natural soil	Pb-contaminated soil
pH	8.2±0.1	7.3±0.1
Moisture (%)	17.6±0.32	20.2±0.45
Organic matter (mg kg^{-1})	17.3±0.12	20.8±0.22
Electrical conductivity (mS m^{-1})	178.0±6.3	1237.1±8.9
Available phosphorus (mg kg^{-1})	40.5±1.1	22.3±0.9
Pb (mg kg^{-1})	24.0±2.2	4985.0±2.6
Mn (mg kg^{-1})	379.0±6.3	632.0±5.8
Cu (mg kg^{-1})	46.0±3.2	36.0±3.1
Zn (mg kg^{-1})	115.0±5.2	82.0±2.6
K (mg kg^{-1})	259.9±12	263.4±13
Cl (mg kg^{-1})	189.0±3.2	165.0±4.3

due to the availability of published data on this [35, 43]. This study is expected to provide a reliable approach for the long-term remediation of lead-contaminated soil.

Materials and Methods

Materials

HAP powder (80 μm particle size) was purchased from Shanghai Macklin Biochemical Co., Ltd. $Pb(NO_3)_2$ and KCl were purchased from Sinopharm Chemical Reagent Co., Ltd. All the reagents were of analytical reagent grade and were used as received. The water used in this study was deionized water unless specified otherwise.

Soil Preparation and Characterization

Genuine polluted soil typically contains various contaminants that may induce side reactions [47]. In order to simplify the reaction process and focus on illustrating the Pb remediation mechanism, simulated Pb-contaminated soil was employed in our experiments. Fresh natural topsoil (0-20 cm depth) was collected from China University of Mining and Technology (117°14′E, 34°21′N, China). After air-drying at 25°C, the soil was sieved through a 2 mm mesh to remove large impurities. A Pb concentration of 4985 mg kg^{-1} was selected to mimic industrially polluted soil in China [48]. Natural soil (500 g, dry weight) was mixed with 200 mL of 12.5 g L^{-1} $Pb(NO_3)_2$ solution. The mixture was subsequently sealed with plastic wrap, rested in a shaded area for 7 days, air-dried under natural sunlight, ground, and sieved through a 100-mesh sieve. The simulated Pb-containing soil samples were acid digested with a mixture of HNO_3, HCl, HF, and $HClO_4$ in a volume ratio of 1:3:3:1 [49]. After that, the Pb concentration in the soil was determined by flame atomic absorption spectrophotometry (FAAS, TAS 990 Super, Persee, China). To ensure the accuracy of FAAS measurements, a method blank and the certified reference material GBW07427 (GSS-13) were analyzed after each set of nine samples, in accordance with ISO/IEC 17025 guidelines. The limit of quantification was considered to be 3 times the limit of detection [50, 51].

Other key performance indicators were evaluated by following established methodologies. The soil pH was measured by the PHS-3E meter (Shanghai INESA Scientific Instrument Co., Ltd., China) at the solid-liquid ratio of 1:2.5 (g mL^{-1}). Soil conductivity was determined by a conductivity meter (AP-2-US, China) at a solid-liquid ratio of 1:5 (g mL^{-1}). Available phosphorus was quantified by spectrophotometry at a solid-liquid ratio of 1:20 (g mL^{-1}). The organic matter content was measured by the volumetric method using potassium dichromate. Moisture content (%) was calculated by drying the soil until constant weight at 105°C for 24 h. Heavy metal content, including Mn, Cu, and Zn, was determined by FAAS after acid digestion with HNO_3-HCl-HF-$HClO_4$. The contents of K and Cl were determined by ion chromatography (ECO IC, Metrohm, Switzerland) after acid digestion. All the tests were performed at 25°C unless otherwise specified. The physical and chemical characteristics of the natural and contaminated soil are presented in Table 1.

Preliminary Tests in Aqueous Solution

In order to determine the optimum molar ratio of remediation materials and to explore the reaction mechanism between HAP, KCl, and Pb^{2+}, preliminary tests were performed in aqueous solution to exclude possible side reactions. Regarding the selection of P:Cl:Pb molar ratio, the P:Pb stoichiometric ratio of the target product $Pb_5(PO_4)_3Cl$ is 0.6:1. To account for side reactions between phosphorus and lead in contaminated soil, an excess of HAP was added. The P:Cl:Pb molar

ratios were eventually set at 0.6:1:1, 0.6:2:1, 1:1:1, 1:2:1, 2:1:1, and 2:2:1, respectively. The Pb concentration in the aqueous solution was maintained at 4985 mg L^{-1}, which is consistent with that in the simulated soil. HAP and KCl were initially added to the Pb-containing solution, and the pH was maintained at 7.3 using either 0.1 M NaOH or 0.1 M HCl. The mixed solution was continuously shaken at 200 rpm (SHA-B, China) at 20℃ ± 2℃ for 28 hours. In the meantime, aqueous samples were withdrawn using a syringe every 2 hours. After 10 minutes of centrifugation (TG16, China, 3000 rcf) and 0.45 μm filtration, the samples were analyzed by FAAS to determine the Pb^{2+} concentration for subsequent removal efficiency evaluation. The precipitates were collected, oven-dried (103-105℃) until constant weight, and finally characterized by X-ray diffractometry (XRD, D8 Advance, Bruker, Germany).

Immobilization Tests in Soil

The P:Cl:Pb molar ratios for the immobilization tests in soil were set at 2:2:1, 4:2:1, 8:2:1, 2:4:1, 8:4:1, 6:6:1, 8:8:1, and 10:10:1, respectively. The Pb-contaminated soil (4985 mg kg^{-1}) without treatment served as the control. Higher content of P and Cl was applied than that in aqueous tests due to the complexity of soil components and potential side reactions. 25 g of Pb-contaminated soil samples (4985 mg kg^{-1}) were thoroughly mixed with weighed amounts of HAP, KCl, and deionized water. The mixtures were incubated at 25℃ for 14 days [52], with the moisture content maintained at 40% ± 2% [53]. At the end of the experiment, 1 g of the soil sample was taken to extract Pb using the toxicity characteristic leaching procedure (TCLP) (HJ/T 300-2007). Additionally, 0.5 g of soil samples were subjected to the European Community Bureau of Reference (BCR) sequential extraction procedure to evaluate different Pb species, including weak acid soluble, reducible, oxidizable, and residual fractions [46, 54, 55]. Further samples were prepared for scanning electron microscopy (SEM, Quanta250, FEI, USA) and XRD analysis to characterize the soil particle morphology and crystal structure of the precipitates, respectively.

Rainfall Exposure

Rainfall experiments were designed with varying SO_4^{2-}:NO_3^- ratios (1:1, 2:1, and 4:1) and pH values to evaluate the long-term stability of remediated soil relevant to East China. These conditions simulated a range of rainfall characteristics, including acid rain (pH 4.5 and 5.6) and neutral rain (pH 6.5). Based on the annual precipitation (~1300 mm) in East China and a soil dry density of 1.30 g cm^{-3} [53, 56, 57], it is estimated that 1 g of dry soil receives approximately 1 mL of rainfall annually. Accordingly, the impact of a 10-year rainfall exposure can be simulated by mixing remediated soil with simulated rainwater at a solid-to-liquid ratio of 1:10 g mL^{-1} [57, 58]. The mixture was shaken at 200 rpm for 8 hours, followed by centrifugation at 300 rpm for 10 minutes (TG16 centrifuge, China) [53]. To simulate a 50-year rainfall cycle, the mixture underwent four additional cycles, each consisting of an 8-hour incubation and a 10-minute centrifugation. Subsequently, the supernatant was collected, and the Pb concentration was analyzed by FAAS. The collected supernatant after 2, 3, 4, and 5 cycles represented the leached Pb over 20, 30, 40, and 50 years of rainfall exposure, respectively. The ultimate 0.5 g of soil after the fifth cycle was subjected to the BCR sequential extraction to evaluate the diverse Pb species after 50 years of simulated rainfall.

Environmental Risk Assessment

The Risk Assessment Code (RAC) was calculated to assess the environmental risks of Pb exposure before and after remediation, and further after the rainfall exposure. Risk levels were divided into 5 levels (Table S1) according to the calculated RAC values [59]. Higher RAC values indicate a higher risk level of Pb exposure.

$$\text{RAC, \%} = \frac{F_1}{F_1 + F_2 + F_3 + F_4} \times 100 \quad (1)$$

where the F_1, F_2, F_3, and F_4 are the respective Pb concentrations of the weak acid soluble, reducible, oxidizable, and residual Pb fractions.

Statistical Analysis

To ensure accuracy and repeatability, all experiments were performed in triplicate, and experimental errors were maintained below 5%. All experimental data were processed using Microsoft Excel 2021 and presented as mean ± standard error. Graphical representations were generated using Origin 2023 software. Experimental data were subjected to analysis of variance (ANOVA) and regression analysis using SPSS 19.0 software (SPSS Inc., Chicago, IL, USA). Mean separation was conducted via the least significant difference (LSD) test at a significance level of $P<0.05$.

Results and Discussion

The Pb Removal in Aqueous Solution

Upon addition of HAP and KCl at a molar ratio of 0.6:1:1 (P:Cl:Pb), the aqueous Pb^{2+} concentration decreased from 4985 mg L^{-1} to 137 mg L^{-1} (97.3% removal efficiency) within 2 hours. Thereafter, equilibrium was established, and the concentration remained constant (Fig. S1a). Analogous trends were observed with increasing HAP and KCl concentrations, such as P:Cl:Pb molar ratios of 0.6:2:1, 1:1:1, 1:2:1, and 2:1:1 (Fig. S1a-S1c). After increasing the ratio to

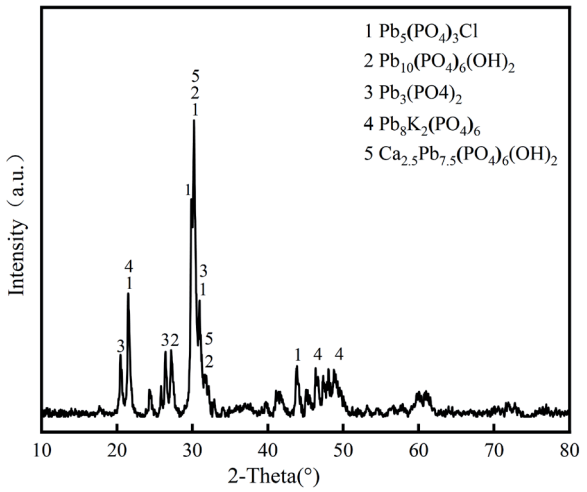

Fig. 1. XRD patterns of precipitates, where the Pb solution (4985 mg L^{-1}, pH = 7.3) was treated with HAP and KCl (P:Cl:Pb = 2:2:1) for 28 hours.

2:2:1, Pb removal efficiency reached 100% within 28 hours (Fig. S1c). This result indicates that when both P and Cl are supplied in excess, the relatively stable intermediate precipitates can further transform into more thermodynamically stable products, leading to complete lead immobilization. Therefore, maintaining an excess of both P and Cl is essential for achieving quantitative lead removal.

Subsequent XRD analysis revealed the primary products such as $Ca_{(10-x)}Pb_x(PO_4)_6(OH)_2$, $Pb_8K_2(PO_4)_6$, $Pb_3(PO_4)_2$, $Pb_{10}(PO_4)_6(OH)_2$, and $Pb_5(PO_4)_3Cl$, with characteristic diffraction peaks at 2θ = 30.107°, 21.782°, 20.861°, 30.099°, and 30.206°, respectively (Fig. 1). The proposed mechanisms for Pb removal using HAP and KCl in aqueous solution are illustrated in Fig. 2: (1) dissolution-precipitation [35, 60-62], HAP initially dissolved, generating $H_2PO_4^-$ and PO_4^{3-} , which subsequently reacted with Pb^{2+}, Cl^-, and K^+ to form precipitates such as $Pb_{10}(PO_4)_6(OH)_2$, $Pb_5(PO_4)_3Cl$, $Pb_3(PO_4)_2$, and $Pb_8K_2(PO_4)_6$; (2) ion exchange [63], wherein some Pb^{2+} was adsorbed onto the HAP surface, partially replacing Ca^{2+} and forming $Ca_{(10-x)}Pb_x(PO_4)_6(OH)_2$; (3) surface complexation [64], some Pb^{2+} was immobilized by ≡POH, ≡PO^-, and/or ≡CaOH, forming predominant complexes on the HAP surface.

The Pb Immobilization in Soil: The Efficiency and Mechanisms

Fig. 3a) shows the Pb leaching concentration and species distribution, before and after soil treatment with HAP and KCl for 14 days. Prior to treatment, the TCLP leached Pb was 563.65 mg kg^{-1}, accounting for 11.3% of the total spiked concentration (4985 mg kg^{-1}). Similar TCLP-Pb proportions of 8.4% and 6.5% were reported by Wang et al. [43] and Shen et al. [53], respectively. This observation can be attributed to the soil preparation method, involving a 7-day incubation with $Pb(NO_3)_2$ followed by air-drying, during which Pb reacted with soil components to form precipitates. Consequently, only 11.3% of the total Pb was leached by the TCLP method. The BCR analysis shows that Pb species are mainly weak acid soluble (31.2%) and reducible Pb (58.7%), which can be easily leached out and transformed into free Pb^{2+} in the natural environment. The other 10.2% existed in oxidizable Pb, while no residual Pb was detected in the control. A similar species distribution was obtained by Liu et al. [46], with 35% weak acid soluble, 55% reducible, 5% oxidizable, and 5% residual Pb.

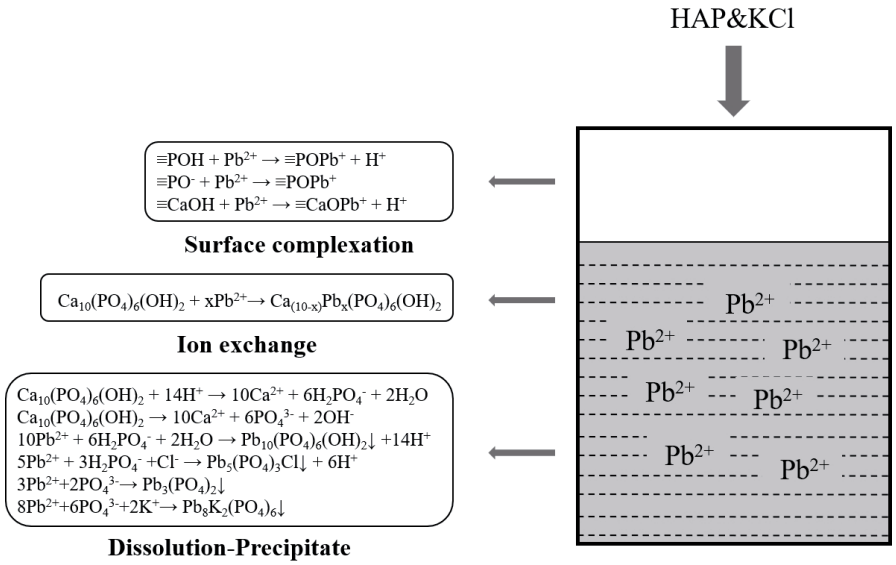

Fig. 2. The proposed Pb (4985 mg L^{-1}) removal mechanisms in aqueous solution using HAP and KCl (P:Cl:Pb = 2:2:1), pH = 7.3.

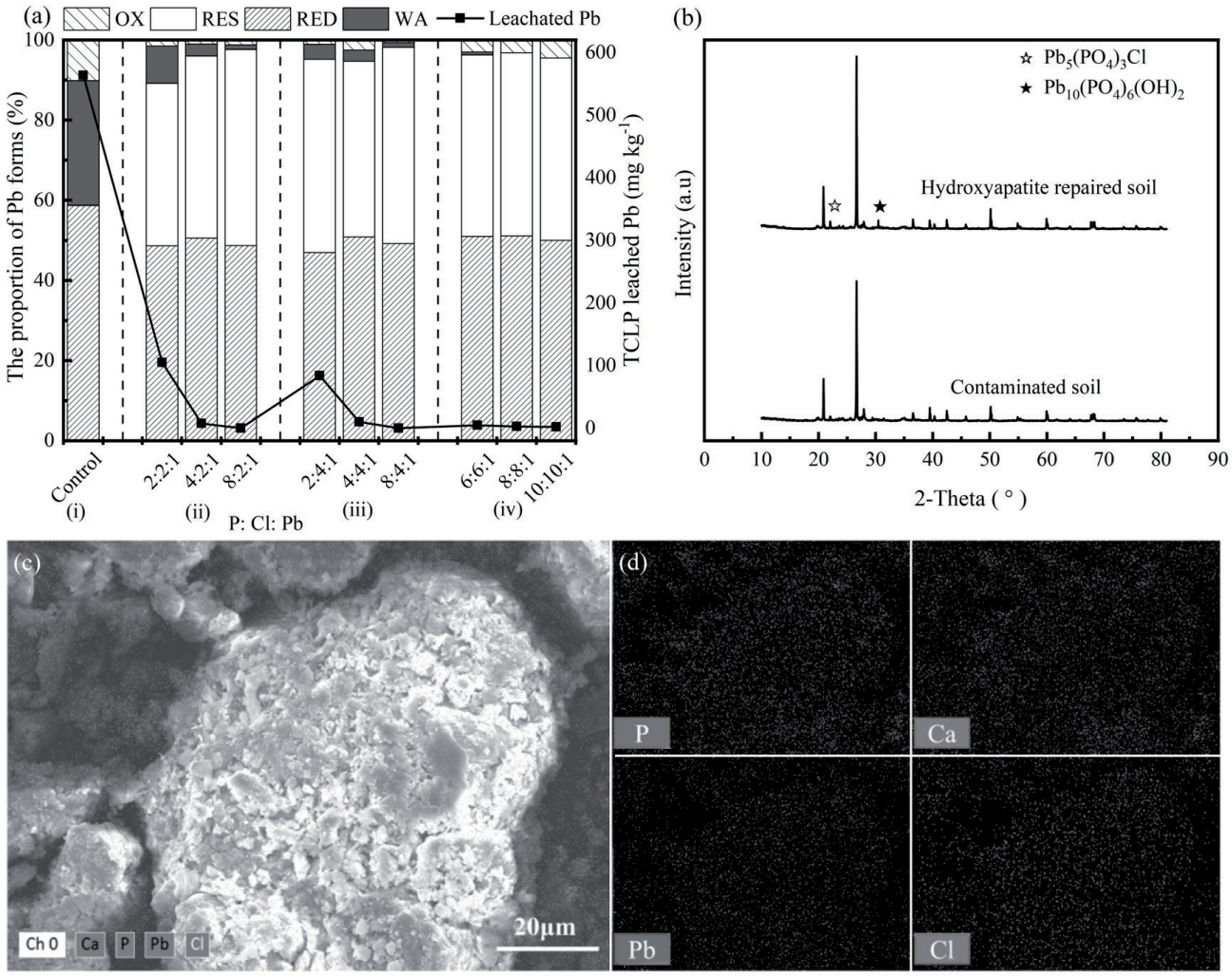

Fig. 3. The full characterization of soil remediated with different mass ratios of HAP and KCl (38%–42% moisture content, 25°C, pH 7.3, 14 days); a) TCLP leached Pb (mg kg^{-1}) concentration and Pb species distribution; b) XRD patterns; c) SEM image; d) EDS data. Note: Control, the Pb-contaminated soil (4985 mg kg^{-1}) without treatment

Treatment with the minimum dosage of HAP and KCl (P:Cl:Pb = 2:2:1) for 14 days reduced the TCLP-Pb concentration from 563.65 mg kg^{-1} to 104.77 mg kg^{-1} (5.24 mg L^{-1}), which is slightly over the regulatory threshold limits of 5 mg L^{-1} (GB 5058.3-2007). Concurrently, the weak acid soluble Pb fraction decreased from 31.2% to 9.3%, reducible Pb reduced from 58.7% to 48.6%, and oxidizable Pb reduced from 10.2% to 1.5%, while the residual Pb increased from 0% to 40.6%. Upon increasing the HAP dosage to P:Cl:Pb = 8:2:1 (3.2 wt% HAP), the TCLP-Pb concentration further diminished to 0 mg kg^{-1}, and the residual Pb fraction further increased to 48.9%. A further increase of the Cl content from 2:1 to 4:1 (Cl:Pb) resulted in a slight decrease in the TCLP-Pb leaching concentrations (Fig. 3a)) and weak acid soluble Pb proportions. Upon further increasing the P:Cl:Pb ratio to 6:6:1, 8:8:1, and 10:10:1, the TCLP-Pb and weak acid soluble Pb fractions were eliminated. These results indicated that increasing chlorine ions can enhance the remediation efficiency of Pb-contaminated soil. However, excessive chloride ions may erode and deteriorate the hydrated products in the soil, adversely affecting the cementation of soil aggregates [40, 42]. The optimum P:Cl:Pb ratio of 8:2:1 (3.2 wt%) with minimum chloride input was therefore selected, and the remediated soil was further analyzed by SEM and XRD to elucidate the Pb immobilization mechanism.

The additive KCl at the optimum ratio (P:Cl:Pb = 8:2:1) dramatically enhanced the generation of the residual state of Pb (49%), compared with HAP-only, HAP-related, and other treatments in Table 2. For example, Wang et al. [35] applied 3% wt HAP-only on slightly contaminated soil (16.12 mg L^{-1} Pb), obtaining only 15% residue state Pb. In terms of the HAP-related materials, Yan et al. [45] found the hydroxyapatite derived from flue gas desulphurization gypsum (FDG-HAP) produced 16.0%-40.2% residual Pb fraction. Yan et al. [44] used DW-HAP (3% wt) derived from distiller waste, yielding a TCLP-Pb of 30 mg kg^{-1} and 30.0% residual Pb. Qian et al. [65] used 5% wt apatite to treat 2647 mg kg^{-1} Pb-contaminated soil for 5 months and

Table 2. Summary of the remediation performance of different agents, including TCLP-Pb and residual Pb. "-" indicates no reliable data available.

Remediation reagents		Control				After remediation			After rainfall		Reference
		Total Pb (mg kg^{-1})	TCLP-Pb (mg kg^{-1})	Leaching rate (%)	Residue state Pb (%)	TCLP-Pb (mg kg^{-1})	Removal rate (%)	Residue state Pb (%)	TCLP-Pb (mg L^{-1})	Residue state Pb (%)	
HAP:KCl:Pb	2:2:1	4985	563.65	11.5	0	104.77	81.4	40.58	-	-	This study
HAP:KCl:Pb, 3.2% wt	8:2:1	4985	563.65	11.5	0	0	100	48.88	3.55	90	This study
HAP:Pb	8:1	1248.67	104.9	8.4	-	24.08	77.04	-	-	-	[43]
		1378.00	120.85	8.7	-	-	-	-	-	-	
HAP	3% wt	-	322.4	-	-	11.96	96	~15	-	-	[35]
	5% wt	-		-	-	-	-	~50	-	-	
HA/A[1]	0.5% wt	800	~220	27.5	~5	~175	20.45	6.16	-	-	[46]
	1% wt					~119	45.91	8.08	-	-	
	2% wt					~91	58.64	12.25	-	-	
HAPs[2], 3% wt	HAP-005	5638	>2000	>35	6.7	38	98.1	32	-	-	[44]
	HAP-05					36	98.2	33	-	-	
HAP/CSH+biochar	10:0	-	185	-	12.37	3.93	97.88	48.82	-	-	[32]
	4:6	-	-	-		14.78	92.01	45.43	-	-	
Apatite	5% wt	-	212	-	-	-		21.8	-	-	[65]
apatite + ferrihydrite	5% wt + 5% wt	-		-	-	108	49.06	41.8	-	-	
MgO	short-term	4280	~280	6.5	-	15–26.2	94.6–90.6	-	-	-	[53]
	long-term		234–328	5.47–7.66	-	39.8–68.6	70.68–87.87	-	-	-	
MgO		736	-	-	-	-	94.84	42	< 0.01	-	[58]
FGD-HAP		-	-	-	7.2	-	-	16.984–40.176	< 0.01	-	[45]
KH_2PO_4		3169	-	-	13.83	540	81.63	25.72	-	-	[66]
SiO_2@Fe_3O_4@C-COOH + TIAs		572.75	21.34	3.7	6.5	3.18	85.10	20.92	-	-	[67]

[1] HA/A is hydroxyapatite/attapulgite composite, n(Ca): n(P) = 5:3.

[2] using Distiller waste (DW) in the production of HAP.

achieved a 21.8% residual state. Further addition of 5 wt% ferrihydrite (composite of 5 wt% apatite and 5 wt% ferrihydrite) increased the residue state to 41.8%. The respective residual Pb generated by other remediation reagents, such as MgO (~42.0%) [58], KH_2PO_4 (25.7%) [66], and SiO_2@Fe_3O_4@C-COOH (20.9%) [67] was also less than that of our combined HAP and KCl.

The weak acid soluble and reducible Pb in soil firstly decomposed to free Pb^{2+}. The introduction of HAP led to the generation of $H_2PO_4^-$ and PO_4^{3-} in the soil, increasing the negative charge on soil particle surfaces, facilitating the uniform adsorption of free Pb^{2+} onto the soil [68]. The addition of KCl contributed to the presence of Cl^- in the soil. Residual Pb, such as $Pb_{10}(PO_4)_6(OH)_2$ and $Pb_5(PO_4)_3Cl$, was subsequently formed by Pb^{2+}, PO_4^{3-}, $H_2PO_4^-$, and Cl^- via dissolution-precipitation and ion exchange [35]. Notably, Cl^- can also react with ettringite present in the soil, leading to the immobilization of a portion of the free Pb^{2+} [42]. The formation of these precipitates was corroborated by XRD analysis of remediated soil in Fig. 3b), exhibiting new characteristic diffraction peaks at 2θ values of 30.457° and 22.015°, respectively. SEM images revealed the presence of uneven and dense flake-like structures (Fig. 3c)) on the surface of the remediated soil, complemented by EDS analysis, which demonstrated similar spatial distributions of Pb, P, and Cl. This suggests the formation of compounds containing P, Cl, and Pb, further confirming the XRD results.

It is noteworthy that 100% of Pb was removed in the aqueous tests (Fig. S1c) at the dosage of P:Cl:Pb = 2:2:1, whilst only 98% of Pb immobilization was achieved in soil treatment under the same dosage conditions. This discrepancy can be attributed to the complex nature of the soil environment, comprising competing ions such as CO_3^{2-}, SO_4^{2-}, OH^-, and various organic matter species, which can interact with HAP and influence its Pb^{2+} immobilization efficiency [69, 70]. Additionally, the uneven distribution of HAP and KCl in soil also hampers Pb immobilization.

The Long-Term Stability under Rainfall Stress

Fig. 4 shows the Pb leaching concentration from soil remediated with HAP and KCl (P:Cl:Pb = 8:2:1) over a simulated 50-year rainfall period. The leached Pb remained below 1 mg L^{-1} during the initial 30 years across all simulated rainfall compositions (SO_4^{2-}:NO_3^- ratios of 1:1, 2:1, and 4:1) and pH levels (4.5, 5.6, and 6.5). A slight increase in Pb leaching was observed over time, reaching a maximum concentration of 3.55 mg L^{-1} (3.6%) at the 50-year mark, which remained below the regulatory threshold value of 5 mg L^{-1} (GB 5058.3-2007). This may be because HAP dispersed into nanoparticles and migrated with leachate under acidic and neutral rainfall, causing a slight decrease in lead immobilization.

Fig. 5 illustrates that the Pb species exhibited dramatically greater stability after 50 years of simulated rainfall exposure. The weak acid soluble and reducible Pb were nearly all transformed to the residual Pb (49% vs 90%) regardless of pH value, with 10% reducible left in the soil. This means that, instead of being dissolved and leached out in acidic and neutral rainfall [71], the weak acid soluble and reducible Pb were transformed into residual fractions by HAP and KCl. This is because the rainfall facilitated the release of $H_2PO_4^-$ from the residual HAP [72], which predominantly reacted with the liberated Pb, forming highly stable residual Pb species, such as $Pb_{10}(PO_4)_6(OH)_2$ ($K_{sp} = 10^{-76.8}$) and $Pb_5(PO_4)_3Cl$ ($K_{sp} = 10^{-84.4}$) [73, 74]. The rates of these reactions were independent of pH. Additionally, the application of HAP could elevate soil pH and enhance the buffering capacity against acidic to neutral rainfall [75]. Only a minimal amount of unreacted Pb was leached out during the initial 30 years, regardless of pH value. This indicates that the P:Cl:Pb dosage ratio of 8:2:1 can ensure excellent long-term remediation performance over 50 years under rainfall environments (pH 4.5-6.5).

Regarding the effect of rainfall composition, it was observed that the maximum Pb leaching concentration decreased from 3.55 mg L^{-1} (SO_4^{2-}:NO_3^- = 1:1) to 2.16 mg L^{-1} (SO_4^{2-}:NO_3^- = 2:1), and further to 1.33 mg L^{-1} (SO_4^{2-}:NO_3^- = 4:1) with the increasing ratio of SO_4^{2-} to NO_3^- (Fig. 4). This trend was further corroborated by the Pb species distribution shown in Fig. 5, where the oxidizable Pb fraction disappeared as the SO_4^{2-}:NO_3^- ratio increased. A possible explanation is the reaction between SO_4^{2-} and the leached Pb^{2+} generated the highly stable $PbSO_4$ precipitates $K_{sp} = 10^{-12.8}$ [76]. Consequently, in regions where the rainfall composition exhibits a higher content of SO_4^{2-}, the combined remediation approach employing HAP and KCl may result in even better performance.

In terms of the effect of rainfall pH, the differences in Pb leachability were primarily observed between years 30 and 50, as the leached Pb concentrations were minimal during the initial years. When the SO_4^{2-}:NO_3^- ratio was 1:1, the maximum Pb leaching concentration was observed at the lowest pH of 4.5 (Fig. 4a)). However, as the SO_4^{2-}:NO_3^- ratio increased to 2:1 and 4:1, the maximum Pb leachability shifted to the medium pH of 5.6 (Fig. 4b) and 4c)). This can be attributed to the interplay between Pb solubility and $PbSO_4$ precipitation. Generally, Pb solubility reaches its peak at the minimum pH of 4.5 [77]. When the SO_4^{2-}:NO_3^- ratio was 1:1, the low pH of 4.5 facilitated the dissolution of $Pb(OH)_2$ and $PbCO_3$, generating soluble Pb^{2+} [78], resulting in the most Pb leachability.

Variations of Risk Assessment Code

Table S2 shows the calculated RAC values at different remediation stages. The RAC was 31% before remediation, indicating a high risk of Pb exposure. The risk was reduced to a low level (1%) after 14 days of remediation with HAP and KCl (P:Cl:Pb = 8:2:1), and further decreased to no risk (0%) after 50 years

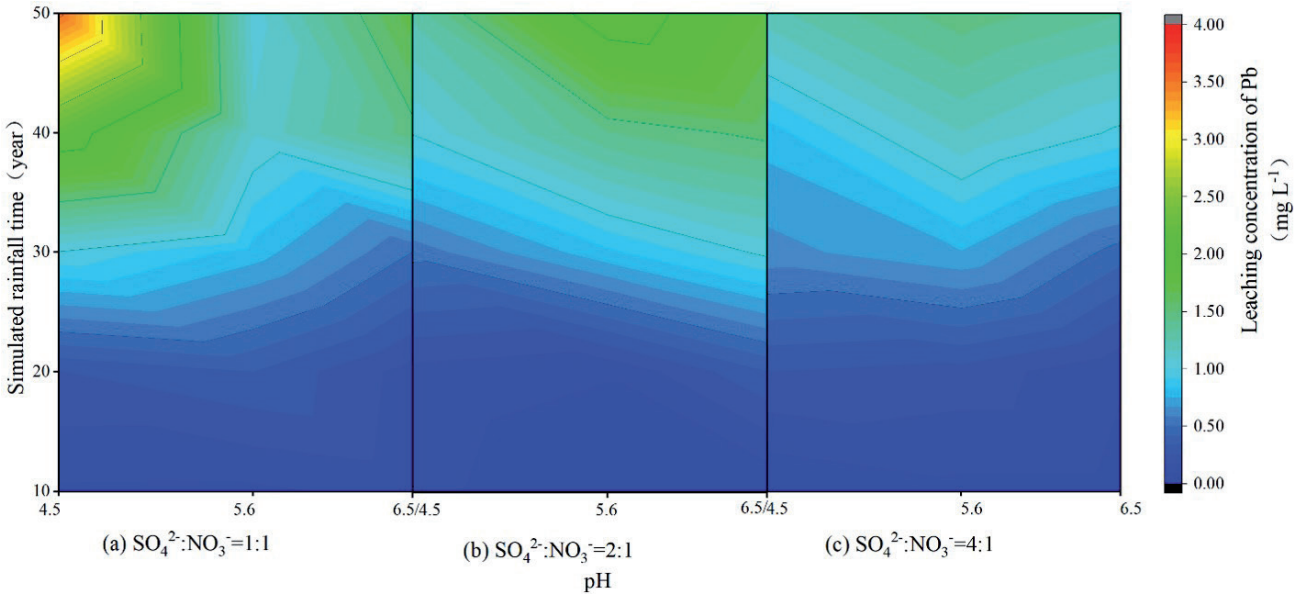

Fig. 4. The Pb leaching concentration from the remediated soil after 50 years of simulation, with different rainfall types and pH values. Note: Before the rainfall simulation, the soil was remediated with HAP and KCl (P:Cl:Pb = 8:2:1) for 14 days. All tests were conducted in triplicate.

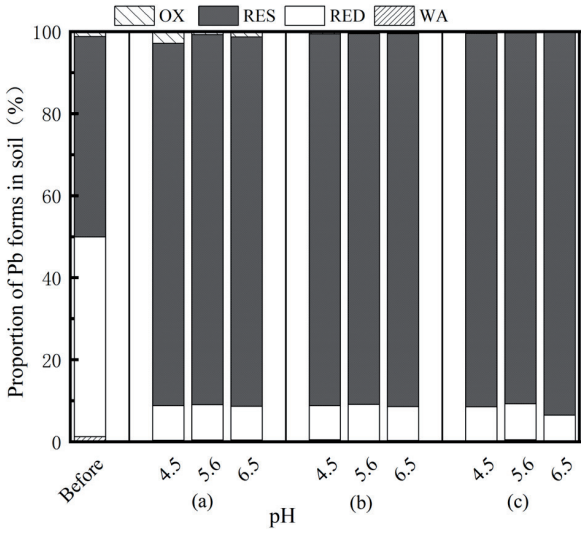

Fig. 5. The distribution of Pb species in the remediated soil (P:Cl:Pb = 8:2:1, 14 days), before and after 50 years rainfall simulation with different pH values and rainfall types: (a) SO_4^{2-}:NO_3^- = 1:1; (b) SO_4^{2-}:NO_3^- = 2:1; (c) SO_4^{2-}:NO_3^- = 4:1. All tests were conducted in triplicates.

of simulated rainfall exposure. This demonstrates that HAP and KCl have great potential in effectively stabilizing Pb in the long run.

Cost Estimation

In terms of the estimated cost, the price of HAP and KCl in the Chinese market ranged between 948-8,487 \$ ton^{-1} and 334-390 \$ ton^{-1} respectively. According to Eqs. (2) and (3), the total combined cost using HAP and KCl (P:Cl:Pb ratio of 8:2:1, 3.2 wt% HAP) is 11.8 \$ m^{-3} soil, comprising 0.3 \$ for KCl (340 \$ ton^{-1}) and 11.5 \$ for HAP (1698 \$ ton^{-1}). It is about half of the cost using HAP only (24.8 \$ m^{-3} soil, 7 wt%), as well as many other reported immobilization methods (about 39.6-205.1 \$ m^{-3}) [14].

$$K_{HAP} = \frac{8 \times C_{Pb}(1\text{-}W) M_{HAP} \times D \times \rho}{3 \times M_{Pb} G_{HAP} \times 10^{11}} \times P_{HAP} \quad (2)$$

$$K_{KCl} = \frac{2 \times C_{Pb}(1\text{-}W) M_{KCl} \times D \times \rho}{M_{Pb} G_{KCl} \times 10^{11}} \times P_{KCl} \quad (3)$$

Where K_{HAP} and K_{KCl} are the costs of HAP and KCl for the remediation of 1 m^3 of Pb-contaminated soil, \$ m^{-3}; C_{Pb} is the lead content in the soil, 4985 mg kg^{-1}; M_{Pb}, M_{HAP}, and M_{KCl} are the respective molecular weights of Pb, HAP, and KCl, g mol^{-1}; D is the depth of lead-contaminated soil, 20 cm; W is the soil moisture content, %; G_{HAP}, G_{KCl} are the purity grades of HAP and KCl, %; ρ is the soil density, 1300 kg m^{-3}; P_{HAP}, PKCl are the prices of HAP and KCl, \$ ton^{-1}.

Conclusions

This study demonstrated the synergistic remediation of lead-contaminated soils using HAP combined with KCl. The optimum P:Cl:Pb molar ratio (8:2:1) offers superior performance, featuring 98% Pb immobilization efficiency, long-term stability with 90% residual Pb under 50-year simulated acidic conditions, and a low cost of 11.8 \$ m^{-3} soil. We believe that the proposed method is a valuable addition to the existing "toolkit" that is available for Pb-contaminated soil. It opens up

the possibility that Pb can be completely immobilized in contaminated soil over the long term, even in acid rain environments. Furthermore, the impact of added chloride on soil physicochemical properties, potential for long-term phosphorus leaching, and the effects of field environmental factors on Pb stabilization should be addressed in the future.

Acknowledgement

This work was supported by the Xuzhou City Frontline Technology R&D Plan for 2025 (Sustainable Development Social Welfare Research, KC25126).

AI Usage Disclosure Statement

During the preparation of this manuscript, the authors used an AI-assisted language editing tool to improve readability and English expression. The authors have reviewed and edited the output and take full responsibility for the content of this publication.

Conflict of Interest

The authors declare no conflict of interest.

Credit Authorship Contribution Statement

Xiangyu Bai: Conceptualization, methodology, writing - review and editing. Xu Xia: Formal analysis, data curation, writing - original draft. Xu Han: Data curation, validation. Wenjing Pan: Conceptualization. Xiaofu Shang: Data curation. Jiachao Jiang: Validation. Dejun Yang: Validation. Gongzhen Li: Conceptualization, methodology. Jun Tian: Conceptualization. Ping Luo: Writing - review and editing, methodology, supervision.

Data Availability

The data will be made available on request.

References

1. KHAN I., IQBAL M., SHAFIQ F. Phytomanagement of lead-contaminated soils: critical review of new trends and future prospects. International Journal of Environmental Science and Technology, **16** (10), 6473, **2019**.
2. ALASMARY Z. Lead (Pb) Contamination in Soil and Plants at Military Shooting Ranges and Its Mitigation Strategies: A Comprehensive Review. Processes, **13** (2), 345, **2025**.
3. AHMED T., NOMAN M., IJAZ M., ALI S., RIZWAN M., IJAZ U., HAMEED A., AHMAD U., WANG Y., SUN G., LI B. Current trends and future prospective in nanoremediation of heavy metals contaminated soils: A way forward towards sustainable agriculture. Ecotoxicology and Environmental Safety, **227**, 112888, **2021**.
4. WYSZKOWSKA J., BOROS-LAJSZNER E., KUCHARSKI J. The Impact of Soil Contamination with Lead on the Biomass of Maize Intended for Energy Purposes, and the Biochemical and Physicochemical Properties of the Soil. Energies, **17** (5), 1156, **2024**.
5. WANG F., YAO J., SI Y., CHEN H., RUSSEL M., CHEN K., QIAN Y., ZARAY G., BRAMANTI E. Short-time effect of heavy metals upon microbial community activity. Journal of Hazardous Materials, **173** (1-3), 510, **2010**.
6. ASHRAF U., KANU A.S., DENG Q., MO Z., PAN S., TIAN H., TANG X. Lead (Pb) Toxicity; Physio-Biochemical Mechanisms, Grain Yield, Quality, and Pb Distribution Proportions in Scented Rice. Frontiers in Plant Science, **8**, 259, **2017**.
7. ORO C.E.D., SAORIN PUTON B.M., VENQUIARUTO L.D., DALLAGO R.M., TRES M.V. Effective Microbial Strategies to Remediate Contaminated Agricultural Soils and Conserve Functions. Agronomy, **14** (11), 2637, **2024**.
8. RAI P.K., LEE S.S., ZHANG M., TSANG Y.F., KIM K.-H. Heavy metals in food crops: Health risks, fate, mechanisms, and management. Environment International, **125**, 365, **2019**.
9. AHMED W., MEHMOOD S., MAHMOOD M., ALI S., NÚÑEZ-DELGADO A., LI W. Simultaneous immobilization of lead and arsenic and improved phosphorus availability in contaminated soil using biochar composite modified with hydroxyapatite and oxidation: Findings from a pot experiment. Environmental Research, **235**, 116640, **2023**.
10. ALABOUDI K.A., AHMED B., BRODIE G. Phytoremediation of Pb and Cd contaminated soils by using sunflower (Helianthus annuus) plant. Annals of Agricultural Sciences, **63** (1), 123, **2018**.
11. RHEE YOUNG J., HILLIER S., GADD GEOFFREY M. Lead Transformation to Pyromorphite by Fungi. Current Biology, **22** (3), 237, **2012**.
12. SHAO Y., YAN T., WANG K., HUANG S., YUAN W., QIN F.G.F. Soil heavy metal lead pollution and its stabilization remediation technology. Energy Reports, **6**, 122, **2020**.
13. CHANG J.-H., WANG Y.-L., DONG C.-D., SHEN S.-Y. The particle-size sieving technique to remediate Pb- and Cu-contaminated agricultural soil. Environmental Geotechnics, **9** (2), 124, **2022**.
14. GONG Y., ZHAO D., WANG Q. An overview of field-scale studies on remediation of soil contaminated with heavy metals and metalloids: Technical progress over the last decade. Water Research, **147**, 440, **2018**.
15. VENGRIS T., BINKIENĖ R., SVEIKAUSKAITĖ A. Electrokinetic remediation of lead-, zinc- and cadmium-contaminated soil. Journal of Chemical Technology & Biotechnology, **76** (11), 1165, **2001**.
16. HUANG K., WANG X., YUAN W., XIE J., WANG J., LI J. Remediation of lead-contaminated soil by washing with choline chloride-based deep eutectic solvents. Process Safety and Environmental Protection, **160**, 650, **2022**.
17. EGENDORF S.P., GROFFMAN P., MOORE G., CHENG Z. The limits of lead (Pb) phytoextraction and possibilities of phytostabilization in contaminated soil: a critical review. International Journal of Phytoremediation, **22** (9), 916, **2020**.

18. PAN X., CHEN Z., LI L., RAO W., XU Z., GUAN X. Microbial strategy for potential lead remediation: a review study. World Journal of Microbiology and Biotechnology, **33** (2), 35, **2017**.
19. LI X., PENG W., JIA Y., LU L., FAN W. Bioremediation of lead contaminated soil with Rhodobacter sphaeroides. Chemosphere, **156**, 228, **2016**.
20. RIGOLETTO M., CALZA P., GAGGERO E., MALANDRINO M., FABBRI D. Bioremediation Methods for the Recovery of Lead-Contaminated Soils: A Review. Applied Sciences, **10** (10), 3528, **2020**.
21. MAHAR A., WANG P., ALI A., GUO Z., AWASTHI M.K., LAHORI A.H., WANG Q., SHEN F., LI R., ZHANG Z. Impact of CaO, fly ash, sulfur and Na2S on the (im)mobilization and phytoavailability of Cd, Cu and Pb in contaminated soil. Ecotoxicology and Environmental Safety, **134**, 116, **2016**.
22. LIANG S.-X., XI X.-C., LI Y.-R. Study of the remediation effects of passivation materials on Pb-contaminated soil. Open Chemistry, **18** (1), 911, **2020**.
23. SONG P., XU D., YUE J., MA Y., DONG S., FENG J. Recent advances in soil remediation technology for heavy metal contaminated sites: A critical review. Science of The Total Environment, **838**, 156417, **2022**.
24. ZHANG X., LOU X. Immobilization of lead and cadmium in soil by sulfide. Chinese Journal of Environmental Engineering, **8**, 782, **2014** [In Chinese].
25. BASTA N.T., MCGOWEN S.L. Evaluation of chemical immobilization treatments for reducing heavy metal transport in a smelter-contaminated soil. Environmental Pollution, **127** (1), 73, **2004**.
26. WILSON C., BRIGMON R.L., KNOX A., SEAMAN J., SMITH G. Effects of Microbial and Phosphate Amendments on the Bioavailability of Lead (Pb) in Shooting Range Soil. Bulletin of Environmental Contamination and Toxicology, **76** (3), 392, **2006**.
27. EL-NAGAR D.A., ABDEL-HALIM K.Y. Remediation of heavy metals in contaminated soil by using nano-bentonite, nano-hydroxyapatite, and nano-composite. Land Degradation & Development, **32** (16), 4562, **2021**.
28. LI Z., ZHOU M.-M., LIN W. The Research of Nanoparticle and Microparticle Hydroxyapatite Amendment in Multiple Heavy Metals Contaminated Soil Remediation. Journal of Nanomaterials, **2014** (1), 168418, **2014**.
29. YANG Z., FANG Z., ZHENG L., CHENG W., TSANG P.E., FANG J., ZHAO D. Remediation of lead contaminated soil by biochar-supported nano-hydroxyapatite. Ecotoxicology and Environmental Safety, **132**, 224, **2016**.
30. YANG Z., GONG H., HE F., REPO E., YANG W., LIAO Q., ZHAO F. Iron-doped hydroxyapatite for the simultaneous remediation of lead-, cadmium- and arsenic-co-contaminated soil. Environmental Pollution, **312**, 119953, **2022**.
31. LIU S., LI H., ZHANG L., HU D., LIU Q. Preparation and characterization of implanted Fe catalyst in hydroxyapatite layer for uniformly dispersion carbon nanotube growth. Applied Surface Science, **455**, 75, **2018**.
32. CHEN H., YUAN X., XIONG T., JIANG L., WANG H., WU Z. Biochar Facilitated Hydroxyapatite/Calcium Silicate Hydrate for Remediation of Heavy Metals Contaminated Soils. Water, Air, & Soil Pollution, **231** (2), 66, **2020**.
33. STÖTZEL C., MÜLLER F.A., REINERT F., NIEDERDRAENK F., BARRALET J.E., GBURECK U. Ion adsorption behaviour of hydroxyapatite with different crystallinities. Colloids and Surfaces B: Biointerfaces, **74** (1), 91, **2009**.
34. MIN M., SHEN L., HONG G., ZHU M., ZHANG Y., WANG X., CHEN Y., HSIAO B.S. Micro-nano structure poly(ether sulfones)/poly(ethyleneimine) nanofibrous affinity membranes for adsorption of anionic dyes and heavy metal ions in aqueous solution. Chemical Engineering Journal, **197**, 88, **2012**.
35. WANG Y., LI R., LIU W., CHENG L., JIANG Q., ZHANG Y. Exploratory of immobilization remediation of hydroxyapatite (HAP) on lead-contaminated soils. Environmental Science and Pollution Research, **26** (26), 26674, **2019**.
36. SELEIMAN M.F., KHEIR A.M.S. Maize productivity, heavy metals uptake and their availability in contaminated clay and sandy alkaline soils as affected by inorganic and organic amendments. Chemosphere, **204**, 514, **2018**.
37. WANG J., SHI L., ZHAI L., ZHANG H., WANG S., ZOU J., SHEN Z., LIAN C., CHEN Y. Analysis of the long-term effectiveness of biochar immobilization remediation on heavy metal contaminated soil and the potential environmental factors weakening the remediation effect: A review. Ecotoxicology and Environmental Safety, **207**, 111261, **2021**.
38. HUANG D., DENG R., WAN J., ZENG G., XUE W., WEN X., ZHOU C., HU L., LIU X., XU P., GUO X., REN X. Remediation of lead-contaminated sediment by biochar-supported nano-chlorapatite: Accompanied with the change of available phosphorus and organic matters. Journal of Hazardous Materials, **348**, 109, **2018**.
39. SCHECKEL K.G., RYAN J.A. Effects of Aging and pH on Dissolution Kinetics and Stability of Chloropyromorphite. Environmental Science & Technology, **36** (10), 2198, **2002**.
40. PONTONI D., FREITAS MELO V., BORGO J., STIPP R., JANICE BONFLEUR E. Integrated assessment of the liquid and solid phases of lead-contaminated soils remediated with phosphate. Geoderma, **360**, 113993, **2020**.
41. MIRETZKY P., FERNANDEZ-CIRELLI A. Phosphates for Pb immobilization in soils: a review. Environmental Chemistry Letters, **6** (3), 121, **2008**.
42. LIU J., ZHA F., XU L., YANG C., CHU C., TAN X. Effect of chloride attack on strength and leaching properties of solidified/stabilized heavy metal contaminated soils. Engineering Geology, **246**, 28, **2018**.
43. WANG L., LI Y., LI H., LIAO X., WEI B., YE B., ZHANG F., YANG L., WANG W., KRAFFT T. Stabilize lead and cadmium in contaminated soils using hydroxyapatite and potassium chloride. Environmental Monitoring and Assessment, **186** (12), 9041, **2014**.
44. YAN Y., QI F., ZHAO S., LUO Y., GU S., LI Q., ZHANG L., ZHOU S., BOLAN N. A new low-cost hydroxyapatite for efficient immobilization of lead. Journal of Colloid and Interface Science, **553**, 798, **2019**.
45. YAN Y., LI Q., YANG J., ZHOU S., WANG L., BOLAN N. Evaluation of hydroxyapatite derived from flue gas desulphurization gypsum on simultaneous immobilization of lead and cadmium in contaminated soil. Journal of Hazardous Materials, **400**, 123038, **2020**.
46. LIU G., LIAO B., LU T., WANG H., XU L., LI Z., YE C. Insight into immobilization of Pb2+ in aqueous solution and contaminated soil using hydroxyapatite/attapulgite composite. Colloids and Surfaces A: Physicochemical and Engineering Aspects, **603**, 125290, **2020**.
47. WANG H., JU C., ZHOU M., CHEN J., KAN X., DONG Y., HOU H. Acid rain-dependent detailed leaching

characteristics and simultaneous immobilization of Pb, Zn, Cr, and Cd from hazardous lead-zinc tailing. Environmental Pollution, **307**, 119529, **2022**.
48. XIONG H., FAN H., GAO J., LIU L. Lead speciation evolution and leaching characteristics of lead contaminated soil solidified and stabilized with phosphorus containing substrate. Environmental Engineering, **37**, 39, **2019** [In Chinese].
49. BAI X., ZHANG M., ZHANG Y., XU Z., JIANG J., LIU X., HU J., LUO P. Ecotoxicological effects of coal fly ash on Daphnia magna: The effect of particulates and leached hazardous trace elements. Desalination and Water Treatment, **324**, 101410, **2025**.
50. FRENTIU T., PONTA M., HATEGAN R. Validation of an analytical method based on the high-resolution continuum source flame atomic absorption spectrometry for the fast-sequential determination of several hazardous/priority hazardous metals in soil. Chemistry Central Journal, **7** (1), 43, **2013**.
51. GEGENSCHATZ S.A., CHIAPPINI F.A., TEGLIA C.M., MUÑOZ DE LA PEÑA A., GOICOECHEA H.C. Binding the gap between experiments, statistics, and method comparison: A tutorial for computing limits of detection and quantification in univariate calibration for complex samples. Analytica Chimica Acta, **1209**, 339342, **2022**.
52. BURTON E.D., LAMB D.T., HAMILTON J., MILLER G., JOHNSTON S.G., KARIMIAN N. Remediation of Pb-contaminated soil using modified bauxite refinery residue. Journal of Hazardous Materials, **437**, 129339, **2022**.
53. SHEN Z., PAN S., HOU D., O'CONNOR D., JIN F., MO L., XU D., ZHANG Z., ALESSI D.S. Temporal effect of MgO reactivity on the stabilization of lead contaminated soil. Environment International, **131**, 104990, **2019**.
54. QI F., LAMB D., NAIDU R., BOLAN N.S., YAN Y., OK Y.S., RAHMAN M.M., CHOPPALA G. Cadmium solubility and bioavailability in soils amended with acidic and neutral biochar. Science of The Total Environment, **610**, 1457, **2018**.
55. SHANG C., CHAI Y., PENG L., SHAO J., HUANG H., CHEN A. Remediation of Cr(VI) contaminated soil by chitosan stabilized FeS composite and the changes in microorganism community. Chemosphere, **327**, 138517, **2023**.
56. LIU X., ZHANG S., ZHANG X., GUO H., LOU Z., ZHANG W., CHEN Z. Cr(VI) immobilization in soil using lignin hydrogel supported nZVI: Immobilization mechanisms and long-term simulation. Chemosphere, **305**, 135393, **2022**.
57. JIANG J., CHEN H., LI Q., XIA X., MA J., WANG L., LUO P. Reduction and immobilization of Cr(VI)-contaminated soil using $FeSO_4$ combined with $(NH_4)_2HPO_4$: The remediation efficiency, mechanisms, and long-term stability. Journal of Environmental Chemical Engineering, **12** (5), 113368, **2024**.
58. SUZUKI T., NAKAMURA A., NIINAE M., NAKATA H., FUJII H., TASAKA Y. Lead immobilization in artificially contaminated kaolinite using magnesium oxide-based materials: Immobilization mechanisms and long-term evaluation. Chemical Engineering Journal, **232**, 380, **2013**.
59. FAN J., BU C., QI Y., ZHOU W., WANG C., WEI Y., SIDDIQUE K.H.M. Biocrusts significantly affect the bioavailability and ecological risk of heavy metals in gold mine tailings. Plant and Soil, **493** (1-2), 99, **2023**.
60. XU H., YANG L., WANG P., LIU Y., PENG M. Kinetic research on the sorption of aqueous lead by synthetic carbonate hydroxyapatite. Journal of Environmental Management, **86** (1), 319, **2008**.
61. DOROZHKIN S.V. Dissolution mechanism of calcium apatites in acids: A review of literature. World Journal of Methodology, **2** (1), 1, **2012**.
62. SESHADRI B., BOLAN N.S., CHOPPALA G., KUNHIKRISHNAN A., SANDERSON P., WANG H., CURRIE L.D., TSANG D.C.W., OK Y.S., KIM G. Potential value of phosphate compounds in enhancing immobilization and reducing bioavailability of mixed heavy metal contaminants in shooting range soil. Chemosphere, **184**, 197, **2017**.
63. BAILLIEZ S., NZIHOU A., BÈCHE E., FLAMANT G. Removal of Lead (Pb) by Hydroxyapatite Sorbent. Process Safety and Environmental Protection, **82** (2), 175, **2004**.
64. MAVROPOULOS E., ROSSI A.M., COSTA A.M., PEREZ C.A.C., MOREIRA J.C., SALDANHA M. Studies on the Mechanisms of Lead Immobilization by Hydroxyapatite. Environmental Science & Technology, **36** (7), 1625, **2002**.
65. QIAN G., CHEN W., LIM T.T., CHUI P. In-situ stabilization of Pb, Zn, Cu, Cd and Ni in the multi-contaminated sediments with ferrihydrite and apatite composite additives. Journal of Hazardous Materials, **170** (2-3), 1093, **2009**.
66. KEDE M.L.F.M., PÉREZ D.V., MOREIRA J.C., MARQUES M. Effect of Phosphates on the Bioavailability and Phytotoxicity of Pb and Cd in Contaminated Soil and Phytoextraction by Vetiver Grass. Journal of Environmental Engineering, **143** (3), 05016008, **2017**.
67. LIU F., SU Y., MA C., XIE P., ZHAO J., ZHANG H. Remediation of Pb-Contaminated Soil Using a Novel Magnetic Nanomaterial Immobilization Agent. Bulletin of Environmental Contamination and Toxicology, **108** (2), 315, **2022**.
68. BOLAN N.S., ADRIANO D.C., NAIDU R. Role of Phosphorus in (Im)mobilization and Bioavailability of Heavy Metals in the Soil-Plant System. In Reviews of Environmental Contamination and Toxicology: Continuation of Residue Reviews, G.W. Ware, L.A. Albert, F. Bro-Rasmussen, D.G. Crosby, P. de Voogt, H. Frehse, O. Hutzinger, F.L. Mayer, D.P. Morgan, D.L. Park, R.S.H. Yang Eds., Springer New York: New York, NY, pp. 1-44, **2003**.
69. PINHEIRO J.P., MOTA A.M., BENEDETTI M.F. Lead and Calcium Binding to Fulvic Acids: Salt Effect and Competition. Environmental Science & Technology, **33** (19), 3398, **1999**.
70. BRADL H.B. Adsorption of heavy metal ions on soils and soils constituents. Journal of Colloid and Interface Science, **277** (1), 1, **2004**.
71. CAO X., MA L.Q., SINGH S.P., ZHOU Q. Phosphate-induced lead immobilization from different lead minerals in soils under varying pH conditions. Environmental Pollution, **152** (1), 184, **2008**.
72. WANG Y., DONG X., CUI J., WEI Z., WANG X. Effect of hydroxyapatite particle size on the formation of chloropyromorphite in anglesite–hydroxyapatite suspensions. RSC Advances, **7** (20), 11896, **2017**.
73. TIBERG C., SJÖSTEDT C., PERSSON I., GUSTAFSSON J.P. Phosphate effects on copper(II) and lead(II) sorption to ferrihydrite. Geochimica et Cosmochimica Acta, **120**, 140, **2013**.
74. DEBELA F., AROCENA J.M., THRING R.W., WHITCOMBE T. Organic acids inhibit the formation of pyromorphite and Zn-phosphate in phosphorous amended Pb- and Zn-contaminated soil. Journal of Environmental

Management, **116**, 156, **2013**.
75. LI H., LIU Y., TANG S., YU Z., CAI X., XU S., CHEN Y., WANG M., WANG G. Mechanisms for potential Pb immobilization by hydroxyapatite in a soil-rice system. Science of The Total Environment, **783**, 147037, **2021**.
76. NOVOSEL B., LJUBIČIĆ P. Methodics of precipitation processes on lead sulfate system in aqueous medium. Colloid and Polymer Science, **256** (10), 1009, **1978**.
77. ELZAHABI M., YONG R.N. pH influence on sorption characteristics of heavy metal in the vadose zone. Engineering Geology, **60** (1-4), 61, **2001**.
78. BADAWY S.H., HELAL M.I.D., CHAUDRI A.M., LAWLOR K., MCGRATH S.P. Soil Solid-Phase Controls Lead Activity in Soil Solution. Journal of Environmental Quality, **31** (1), 162, **2002**.

Supplementary Data

https://www.pjoes.com/SuppFile/220561/1/